Journal of Thermal Science Vol.28, No.3 (2019) 431−441

**https://doi.org/10.1007/s11630-019-1130-8** **Article ID: 1003-2169(2019)03-0431-11**

# Single-Reheating or Double-Reheating, Which is Better for S-$CO_2$ Coal Fired Power Generation System?

**SUN Enhui[1], XU Jinliang[1,2*], HU Han[1], YAN Chenshuai[1], LIU Chao[1]**

1. Beijing Key Laboratory of Multiphase Flow and Heat Transfer for Low Grade Energy Utilization, North China Electric Power University, Beijing 102206, China
2. Key Laboratory of Condition Monitoring and Control for Power Plant Equipment of Ministry of Education, North China Electric Power University, Beijing 102206, China



**Abstract:** The objective of this paper is to provide the optimal choice of single-reheating or double-reheating when considering residual flue gas heat in S-$CO_2$ coal fired power system. The cascade utilization of flue gas energy includes three temperature levels, with high and low temperature ranges of flue gas heat extracted by S-$CO_2$ cycle and air preheater, respectively. Two methods are proposed to absorb residual flue gas heat $Q_{re}$ in middle temperature range. Both methods shall decrease $CO_2$ temperature entering the boiler $T_4$ and increase secondary air temperature $T_{sec\ air}$, whose maximum value is deduced based on energy conservation in air preheater. The system is analyzed incorporating thermodynamics, boiler pressure drop and energy distribution. It is shown that at a given main vapor temperature $T_5$, the main vapor pressure $P_5$ can be adjusted to a value so that $Q_{re}$ is completely eliminated, which is called the main vapor pressure adjustment method. For this method, single-reheating is only available for higher main vapor temperatures. The power generation efficiency for single-reheating is obviously higher than double-reheating. If residual flue gas heat does exist, a flue gas heater FGC is integrated with S-$CO_2$ cycle, which is called the FGC method. Both single-reheating and double-reheating share similar power generation efficiency, but single-reheating creates less residual flue gas heat. We conclude that single-reheating is preferable, and the pressure adjustment method achieves obviously higher power generation efficiency than the FGC method.

**Keywords: S-$CO_2$ coal fired power system, thermodynamics, heat transfer, reheating, residual flue gas heat**

## 1. Introduction

Supercritical carbon dioxide Brayton cycle (S-$CO_2$ cycle) has been extensively investigated for advanced power generation systems using nuclear energy, solar energy and waste heat as the heat sources [1-9]. Compared to Rankine cycle, the S-$CO_2$ Brayton cycle offers various benefits. First, at similar turbine inlet temperature in the range of 550°C−700°C, the cycle efficiency is higher than a water-steam Rankine cycle [10]. Second, $CO_2$ is inert to induce weak corrosion reaction between $CO_2$ vapor and metal material at high temperatures [11,12]. Third, because the whole S-$CO_2$ power system operates at supercritical or near-critical

Received: Dec 14, 2018 Corresponding author: XU Jinliang E-mail: xjl@ncepu.edu.cn

**Nomenclature**

| | | | |
|---|---|---|---|
| $d$ | tube inside diameter/mm | RH | reheat |
| $f$ | frictional coefficient | T | turbine |
| $g$ | gravitational acceleration | **Subscripts** | |
| $h$ | specific enthalpy/kJ·kg$^{-1}$ | 1, 2, 3... | state points of top cycle |
| $l$ | tube length/m | AP | air preheater |
| $m$ | mass flow rate/kg·s$^{-1}$ | b | boiler |
| $P$ | Pressure/MPa | ex | exhaust |
| $Q$ | heat capacity/MW | fg | flue gas |
| $Re$ | Reynolds number | p | pinch |
| $s$ | tube spacing | re | residual |
| $T$ | Temperature/°C | s | isentropic |
| $u$ | flow velocity/m·s$^{-1}$ | sec | secondary |
| **Abbreviation** | | fefg | flue gas temperature at furnace exit |
| C | compressor | **Greek symbols** | |
| DRH | double reheat | $\alpha$ | excess air ratio |
| FGC | flue gas cooler | $\rho$ | density/kg·m$^{-3}$ |
| HTR | high temperature recuperator | $\eta_{th}$ | thermal efficiency |
| LTR | low temperature recuperator | $\eta_b$ | boiler efficiency |
| MS | molten salt | $\eta_p$ | pipeline efficiency |
| RC | recompression cycle | $\eta_g$ | power generator efficiency |
| S-$CO_2$ | supercritical carbon dioxide | $\eta_e$ | power efficiency |

pressure, the system becomes more compact, while a Rankine cycle operates some components such as condenser in vacuum pressure to expand the system size [11,13].

Coal fired power plant provides about 39.3% of the total electricity supply in the world [14]. According to the British Petroleum (BP) statistics, mankind can still use coal for power generation for 153 years, which is longer than other fossil energies of oil and natural gas [15]. The coal fired power generation system plays an important role in the world electricity market for nearly one century [16]. The coal fired power generation using S-$CO_2$ cycle is a new attempt to use coal efficiently and cleanly.

The S-$CO_2$ coal fired power generation is studied in recent years. There are two key issues. The $CO_2$ mass flow rate can be ~9 times of that for a water-steam Rankine cycle, resulting in extremely large boiler pressure drop [17]. Recently, Xu et al. [17] proposed the partial flow strategy to yield module boiler design. The boiler pressure drop is reduced according to the 1/8 principle compared to conventional one-through boiler design. This strategy is coupled with the thermodynamics analysis in this paper.

The extraction of flue gas heat over the entire temperature range is another issue to be overcome [18]. Usually, S-$CO_2$ cycle is suitable for moderate/high temperature heat resource. Applying reheating in the cycle improves the cycle efficiency, but raises the $CO_2$ temperature entering the boiler to make the residual flue gas heat absorption difficult. A flue gas cooler (FGC) can extract residual flue gas heat [17, 19-24]. In such an integration, a small $CO_2$ flow rate is extracted from a coldest point of the cycle (e.g., compressor outlet), heated by flue gas in tail flue, and returns to the cycle (e.g., inlet of a recuperator heat exchanger).

The extraction of residual flue gas heat is related to if single-reheating or double-reheating is used. Refs. [19-21] prefer to use single-reheating. Hanak et al. [19] showed that single-reheating is preferable. Using an additional heating has a slight efficiency improvement but causes a cost penalty. For single reheating S-$CO_2$ coal fired power plant, Zhou et al. [20] indicated an overall exergy efficiency of 45.4%, which is ~3.5% higher than a supercritical water-steam Rankine cycle power plant. On the other hand, Refs. [22-24] prefer to use double-reheating. Moullec Y [22] indicated that double-reheating not only improves cycle efficiency but also keeps better heat transfer performance in boiler. Mecheri et al. [23]

showed that a S-$CO_2$ coal fired power system with double-reheating can have an overall efficiency of 47.8%, which is higher than the highest efficiency of 45% for commercial supercritical water-steam cycle power plant. The above discussion shows that even though many authors integrated single-reheating or double-reheating with S-$CO_2$ cycle, the relationship between residual flue gas heat extraction and reheating is not known.

In this paper, we attempt to answer the question that which one is better for single-reheating or double-reheating for S-$CO_2$ coal fired power system. This paper is organized as follows. Section 2 describes the mathematical model incorporating thermodynamics, boiler pressure drop and energy distribution in the system. Section 3 deals with maximum secondary air temperature. Sections 4 and 5 describe main vapor pressure adjustment method and FGC method, respectively. For both methods, the effect of single-reheating and double-reheating on system performance is paid attention. It is concluded that single-reheating is better than double-reheating, and the main vapor pressure adjustment method is promising for flue gas energy extraction over the entire temperature range.

## 2. Mathematical Model

Fig. 1(a) shows S-$CO_2$ cycle, including C1 (compressor 1), C2 (compressor 2), HTR (high temperature recuperator heat exchanger), LTR (low temperature recuperator heat exchanger), cooler 1, T1 (turbine 1), T2 (turbine 2), T3 (turbine 3), and three heaters corresponding to three turbines. There are four valves V1-V4. The thermal system operates at different modes by switching on/off the four valves. The system becomes S-$CO_2$ recompression cycle (RC) with V1 on and other valves off, S-$CO_2$ recompression + singe-reheating cycle (RC+RH) with V2, V3 on and V1, V4 off, S-$CO_2$ recompression + double-reheating cycle (RC+DRH) with V2, V4 on and V1, V3 off, respectively.

For S-$CO_2$ coal fired power plant, the extraction of residual flue gas heat is important. It is necessary to define and estimate residual flue gas heat. Fig. 1(b)

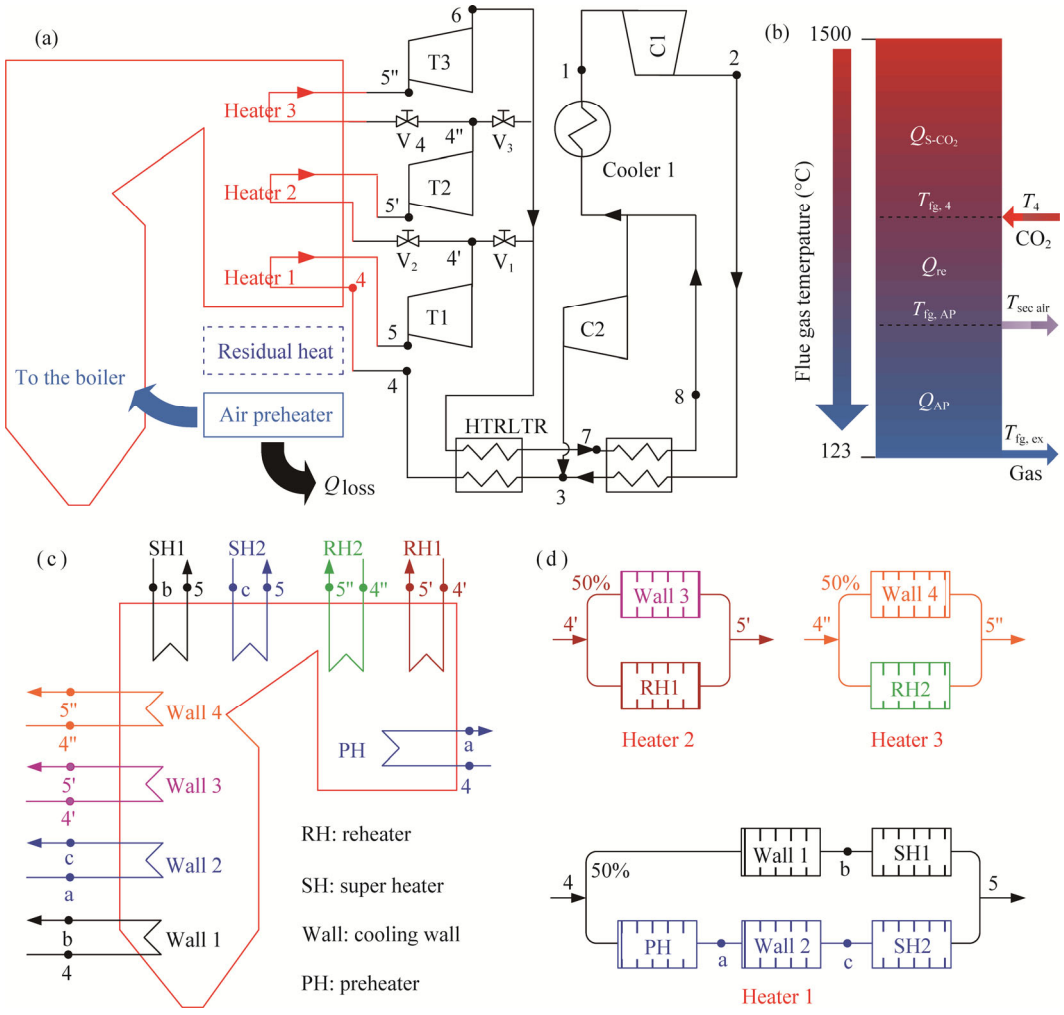


**Fig. 1** S-$CO_2$ coal fired power generation system

shows the cascade utilization of flue gas energy over the entire temperature range. There are three temperature regimes. The high temperature regime of flue gas energy is extracted by S-$CO_2$ cycle, in which $T_4$ is the $CO_2$ temperature entering the boiler; $T_{fg,4}$ is the flue gas temperature correspondingly. Air preheater receives the low temperature flue gas heat, in which $T_{fg,AP}$ is the flue gas temperature entering air preheater. Thus, residual flue gas heat $Q_{re}$ is defined based on the temperature difference between $T_{fg,4}$ and $T_{fg,AP}$, belonging to middle temperature regime.

### 2.1 Thermodynamic model incorporating boiler thermal-hydraulic feature

The thermodynamics computation is based on energy conservation in various components in the cycle. A comprehensive software code is developed using FORTRAN language. Physical properties of $CO_2$ come from REFPROP [25]. Table 1 summarized various parameters for such analysis.

**Table 1** S-$CO_2$ cycle parameters considering boiler pressure drop and energy distribution in boiler

| Parameters | Values |
|---|---|
| turbine inlet temperature ($T_5$) | 475–640°C |
| turbine inlet pressure ($P_5$) | 20–50 MPa |
| turbine isentropic efficiency ($\eta_{t,s}$) | 93% |
| compressor C1 inlet temperature ($T_1$) | 32°C |
| compressor C1 inlet pressure ($P_1$) | 7.6 MPa |
| compressors isentropic efficiency ($\eta_{c,s}$) | 89% |
| pressure drops in LTR and HTR ($\Delta P$) | 0.1 MPa |
| LTR and HTR pinch temperature difference ($\Delta T_{LTR}$ or $\Delta T_{HTR}$) | 10°C |
| primary air temperature ($T_{pri\ air}$) | 320°C |
| primary air temperature at the inlet of air preheater ($T_{pri\ air,in}$) | 31°C |
| ratio of primary air flow rate to the total air flow rate | 19% |
| secondary air temperature ($T_{sec\ air}$) | 400–500°C |
| secondary air temperature at the inlet of air preheater ($T_{sec\ air,in}$) | 21°C |
| secondary air flow rate ratio | 81% |
| excess air coefficient ($\alpha$) | 1.2 |
| exit flue gas temperature ($T_{fg,\ ex}$) | 123°C |
| environment temperature | 20°C |
| pinch temperature between $T_{fg,4}$ and $T_4$ ($\Delta T_{p,4}$) | 40°C |
| pipeline efficiency ($\eta_p$) | 99% |
| power generator efficiency ($\eta_g$) | 98.5% |

Isentropic efficiency and power output for each turbine are

$$\eta_{t,s}=\frac{h_{t,in}-h_{t,out}}{h_{t,in}-h_{t,out,s}},\ W_t=m_t\left(h_{t,in}-h_{t,out}\right) \tag{1}$$

Similarly, for each compressor, we have

$$\eta_{c,s}=\frac{h_{c,out,s}-h_{c,in}}{h_{c,out}-h_{c,in}},\ W_c=m_c\left(h_{c,out}-h_{c,in}\right) \tag{2}$$

In Eqs.(1-2), the subscripts t and c represent turbine and compressor, respectively; in and out mean inlet and outlet, respectively; s stands for isentropic condition, and $h$ stands for enthalpy.

The heat absorption $Q_h$ by heater and heat dissipated by cooler $Q_c$ are

$$Q_h=m_{CO_2,h}\left(h_{h,out}-h_{h,in}\right) \tag{3}$$

$$Q_c=m_{CO_2,c}\left(h_{c,in}-h_{c,out}\right) \tag{4}$$

where $m_{CO_2,h}$ and $m_{CO_2,c}$ are the $CO_2$ mass flow rate in heater and cooler, respectively.

The heat transfer rate is balanced across hot side h and cold side c of HTR or LTR as

$$m_{CO_2,h}\left(h_{h,in}-h_{h,out}\right)=m_{CO_2,c}\left(h_{c,out}-h_{c,in}\right) \tag{5}$$

The cycle thermal efficiency is

$$\eta_{th}=\frac{W_t-\sum W_c}{Q_h} \tag{6}$$

For RC+RH, the intermediate pressure $P_{5'}$ at the inlet of T2 has the relationship with $P_5$ and $P_6$ as [17]

$$P_{5'}=\sqrt{P_5P_6} \tag{7}$$

where $P_5$ is the pressure at the T1 inlet and $P_6$ is the pressure at the T3 outlet.

For RC+DRH, similar relationship between various pressures is [17]

$$P_{5'}=\sqrt[3]{P_5^2P_6},\quad P_{5''}=\sqrt[3]{P_5P_6^2} \tag{8}$$

Eqs. (1-8) deal with thermodynamics analysis. The thermodynamic analysis is incorporated with the pressure drops in each component of the S-$CO_2$ boiler. For a general consideration, the frictional pressure drop $\Delta P_f$ and gravity pressure drop $\Delta P_g$ are written as

$$\Delta P_f=f\frac{1}{2}\frac{l}{d_i}\rho_{CO_2}u_{CO_2}^2=f\frac{1}{2}\frac{l}{d_i}\left(\frac{4}{\pi d_i^2}\right)^2\frac{m_{co_2}^2}{\rho_{CO_2}} \tag{9}$$

where $l$ is the tube length of cooling wall; $d_i$ is the inner diameter; $\rho$ is the density; $m$ is the mass flow rate; $f$ is the friction factor which is given by Filonenko [26].

$$f=\left[1.82\lg\left(Re\right)-1.64\right]^{-2} \tag{10}$$

The tube length $l$ is determined by the energy balance as

$$l=\frac{c_{p,CO_2}m_{co_2}\left(T_{out}-T_{in}\right)}{qs} \tag{11}$$

where $c_p$ is the specific heat; $q$ is the comprehensive heat flux including radiation component and convective component, and $s$ is the distance between two centerlines of neighboring tubes of cooling wall. $\Delta P_g$ is calculated by

$\Delta P_g = \rho_{CO_2} g l$ , where $g$ is the gravitational acceleration.

In our recent study, it is shown that cycle performance is strongly dependent on $CO_2$ pressure in various components of the cycle [17]. Especially, when S-$CO_2$ cycle is used, the $CO_2$ cycling mass flow rate is obviously large to yield large pressure drops in heaters, deteriorating cycle efficiency. In order to significantly decrease pressure drops in heaters, Xu et al. [17] and Sun et al. [18] proposed the partial flow strategy and module boiler design, which are incorporated in this paper. The partial flow strategy cuts a total tube length $l$ with a total mass flow rate $m$ (full flow mode) into two parallel tubes each having a length of $0.5l$ and mass flow rate of $0.5m$ (partial flow mode). It is seen from Eq. (9) that the friction pressure drop is reduced to 1/8 of that for full flow mode. Based on this method, the specific boiler heating surface arrangement is shown in Fig. 1(c). Walls 1-4 are the cooling walls; SH, RH, PH mean superheater, reheater, preheater (economizer) respectively. Heater 1 consists of two parallel streamlines, with one line of Wall 1 and SH1 and the other line of PH, Wall 2 and SH2. Each line has 50% of the total flow rate. Similar arrangements are made for Heaters 2 and 3 (see Fig. 1(d)). We majorly calculate the pressure drops in cooling walls. Usually, for large scale S-water cycle power plant, the cooling wall accounts for nearly half of the total boiler pressure drop. Thus, the pressure drops in the three heaters are $\Delta P_{4\text{-}5}=2\Delta P_{\text{f,Wall 1}}+\Delta P_{\text{g,4-5}}$, $\Delta P_{4'\text{-}5'}=\Delta P_{\text{f,Wall 3}}+\Delta P_{\text{g,4'-5'}}$, $\Delta P_{4''\text{-}5''}=\Delta P_{\text{f,Wall 4}}+\Delta P_{\text{g,4''-5''}}$.

### 2.2 The flue gas energy distribution in boiler

The residual flue gas heat is calculated as (see Fig. 1)

$$Q_{re} = m_{fg}\left(h_{T_{fg,4}} - h_{T_{fg,AP}}\right) \tag{12}$$

where $m_{fg}$ is the flue gas mass flow rate, which is the sum of the coal consumption rate $m_{coal}$ and the mass flow rate of air $m_{air}$ ($m_{fg}=m_{coal}+m_{air}$), $m_{coal}$ is

$$m_{coal} = \frac{Q_h}{\eta_b Q_f} \tag{13}$$

where $Q_h$ is total heat received by S-$CO_2$ cycle (see Eq. (3)), $Q_f$ is the lower heating value of coal ($Q_f$=23442 kJ/kg, see Table 2 for coal parameters), and $\eta_b$ is the boiler efficiency [27]:

$$\eta_b = 1 - \sum_{i=2}^{6} q_i / 100 \tag{14}$$

where $q_i$ is the heat loss. Heat losses due to incomplete chemical combustion ($q_3$), unburned carbon ($q_4$), furnace exterior heat transfer ($q_5$), and sensible heat of ash and slag ($q_6$), are $q_3$=0, $q_4$=0.6, $q_5$=0.2 and $q_6$=0.06, respectively. The heat loss due to exhaust gas ($q_2$) has the dominant contribution to the boiler efficiency, which is

$$q_2 = \frac{\left(h_{T_{fg,ex}} - \alpha h_{air}\right)\left(1 - q_4/100\right)}{Q_f} \times 100 \tag{15}$$

where $\alpha$ is the excess air ratio; $h_{air}$ is the air enthalpy at environment temperature. The power generation efficiency $\eta_e$ is

$$\eta_e = \eta_b \eta_{th} \eta_p \eta_g \tag{16}$$

where $\eta_p$ is the pipeline efficiency and $\eta_g$ is the generator efficiency (see Tab.1 for the values).

## 3. Maximum Secondary Air Temperature

There are two methods to overcome the issue of residual flue gas heat (see Fig. 1):

***The parameters adjustment method:*** If one decreases $T_{fg,4}$ and increases $T_{fg,AP}$ to equalize the two temperatures ($T_{fg,4}=T_{fg,AP}$, see Eq. (12)), residual flue gas heat does not exist. The three regimes of flue gas energy extraction become two regimes. Because $T_{fg,4}$ is related to $T_4$ in Eq. (17), the parameters adjustment method shall adjust both the S-$CO_2$ cycle parameters and the air preheater parameters, which will be analyzed in Section 4.

***The FGC method:*** When $T_{fg,4}$ and $T_{fg,AP}$ are different, a FGC is needed to recover the residual flue gas heat, which will be analyzed in Section 5.

For both methods, residual flue gas heat becomes small if $T_{fg,4}$ is decreased and $T_{fg,AP}$ is increased. $T_{fg,4}$ and $T_4$ ($CO_2$ temperature entering the boiler) are related by a pinch temperature difference:

$$T_{fg,4} = T_4 + \Delta T_{p,4} \tag{17}$$

Similarly, $T_{fg,AP}$ and $T_{sec\ air}$ (secondary air temperature) are related by another pinch temperature:

$$T_{fg,AP} = T_{sec\ air} + \Delta T_{p,air} \tag{18}$$

For our analysis, $\Delta T_{p,4}$=40°C, $\Delta T_{p,air}$ can be calculated by energy conservation equation in air preheater. In order to decrease residual flue gas heat, $T_{fg,AP}$ and $T_{sec\ air}$ should be raised. One may ask a question that *what is the maximum secondary air temperature?* Fig. 2 shows the working principle of an air preheater, including three sectors: a flue gas sector, a primary air sector, and a

**Table 2** Properties of the designed coal

| $C_{ar}$/% | $H_{ar}$/% | $O_{ar}$/% | $N_{ar}$/% | $S_{ar}$/% | $A_{ar}$/% | $M_{ar}$/% | $V_{daf}$/% | $Q_f$/ kJ·kg$^{-1}$ |
|---|---|---|---|---|---|---|---|---|
| 61.70 | 3.67 | 8.56 | 1.12 | 0.60 | 8.80 | 15.55 | 34.73 | 23442 |

*C* (carbon), *H* (hydrogen), *O* (oxygen), *N* (nitrogen), *S* (sulfur), *A* (ash), *M* (moisture), *V* (Volatile).
Subscripts *ar*, *daf* means as received, dry and ash free, $C_{ar}+H_{ar}+O_{ar}+N_{ar}+S_{ar}+A_{ar}+M_{ar}$=100.

secondary air sector. The total air flow rate is divided into two streams: one for primary air and the other for secondary air. Both air streams are heated by flue gas. Usually, the temperatures of primary air and secondary air are different. The primary air temperature is related to the type of coal. For bituminous coal, this temperature is ~300°C [28]. The secondary air provides sufficient oxygen to maintain stable combustion [27]. The secondary air temperature cannot be too high. The energy conservation equation is written for an air preheater as

$$\begin{aligned} & m_{\mathrm{fg}} c_{\mathrm{p,fg}} \left(T_{\mathrm{fg,AP}} - T_{\mathrm{fg,ex}}\right) \\ & = 0.81 m_{\mathrm{air}} c_{p,\mathrm{air}} \left(T_{\mathrm{sec\ air}} - T_{\mathrm{sec\ air,in}}\right) \\ & + 0.19 m_{\mathrm{air}} c_{p,\mathrm{air}} \left(T_{\mathrm{pri\ air}} - T_{\mathrm{pri\ air,in}}\right) \end{aligned} \tag{19}$$

Eq. (19) is rewritten as

$$\begin{aligned} T_{\mathrm{sec\ air}} = & \frac{1}{1-0.81R}\left(T_{\mathrm{fg,ex}} - \Delta T_{p,\mathrm{air}}\right) \\ & - \frac{0.19}{1-1/(0.81R)}\left(T_{\mathrm{pri\ air}} - T_{\mathrm{pri\ air,in}}\right) \\ & + \frac{T_{\mathrm{sec\ air,in}}}{1-1/(0.81R)} \end{aligned} \tag{20}$$

where $T_{\mathrm{fg,ex}}$=123°C (exit flue gas temperature); $T_{\mathrm{pri\ air}}$ is the primary air temperature; $T_{\mathrm{pri\ air,in}}$ is the primary air temperature at the air preheater inlet; $T_{\mathrm{sec\ air,in}}$ is the secondary air temperature at the air preheater inlet, and $R=m_{\mathrm{air}}c_{\mathrm{p,air}}/(m_{\mathrm{fg}}c_{\mathrm{p,fg}})$.

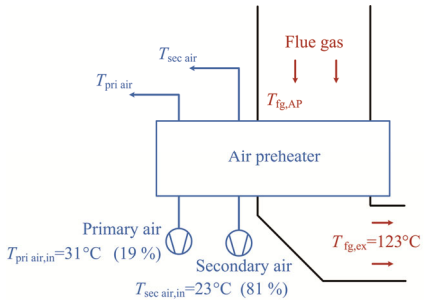


**Fig. 2** Tri-sector rotary air preheater

Eq. (20) shows $T_{\mathrm{sec\ air}}$ as a function of $R$, which is the mass flow rate ratio of air to flue gas multiplying the specific heat ratio of air to flue gas. When both coal and excess air coefficient are given such as shown in Tabs.1-2, $m_{\mathrm{air}}/m_{\mathrm{fg}}$ is a specific value. Specific heat is weakly dependent on temperatures for air and flue gas. Fig. 3(a) shows enthalpies of air and flue gas versus temperatures. The larger slope of enthalpies versus temperatures for flue gas than those for air, indicates larger specific heat of flue gas than air. The difference of enthalpies between the two fluids is increased with increase of temperatures. Fig. 3(b) shows flue gas temperatures versus secondary air temperatures. The flue gas temperatures are quasi-linearly approaching the secondary air temperatures, until $T_{\mathrm{fg,AP}}$ equals to $T_{\mathrm{sec\ air}}$ at 531.9°C, which is the maximum secondary air temperature with zero pinch temperature in air preheater.

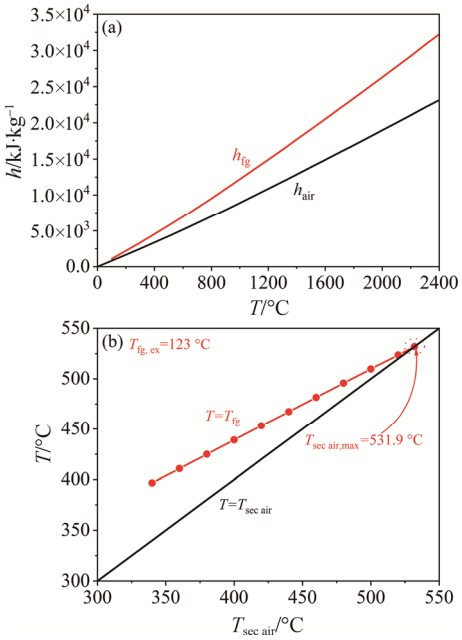


**Fig. 3** Enthalpies of flue gas and air (a) and flue gas temperatures versus secondary air temperatures (b)

However, can the secondary air temperature approach this maximum value? There are two limitations which should be noted. The first limitation refers to relatively small heat transfer coefficient in air preheater, leading to the rise of air preheater volume with increase of $T_{\mathrm{sec\ air}}$. This reason limits the application of tri-sector rotary air preheaters due to the dramatic mushroom droopy deformation of rotor [29]. This issue can be solved by modifying the air preheater, see Fig. 4 for two possible arrangements of the high-temperature air preheater regarding its modification.

The first type combines the molten salt air preheater and rotary air-preheater (see Fig. 4(a)). The second type combines the tube air preheater and rotary air-preheater (see Fig. 4(b)). For both of them, the low-temperature flue gas heat can be absorbed by a rotary air preheater, similar to a large-scale tri-sector rotary air preheater. The high-temperature flue gas heat can be absorbed by the molten salt air preheater (the first type) and tube air preheater (the second type) respectively. The air temperature can be further increased via the above modifications.

The second limitation is that the additional heat of air added in the furnace may highly increase the flue gas temperature at furnace exit ($T_{\mathrm{fefg}}$), which may cause a severe damage to the superheater. Based on this problem, the relationship between $T_{\mathrm{fefg}}$ and $T_{\mathrm{sec\ air}}$ has been explored according to the boiler design standard [30].

Here, the furnace exit is defined at the furnace arch. We show that with increase of $T_{\text{sec air}}$ from 320°C to 520°C, $T_{\text{fefg}}$ is slightly increased from 1298.6°C to 1305.1°C. The small increment of $T_{\text{fefg}}$ within 6.5°C has weak effect on the superheater due to the following two reasons. The first reason is that with increase of $T_{\text{sec air}}$, the thermal efficiency of the S-$CO_2$ cycle is increased to decrease the coal consumption rate at the same power output (see Fig. 5(a)). The second reason is that with increase of $T_{\text{sec air}}$, the theoretical flame temperature will be increased because additional heat of air is added in the furnace, elevating the thermal load of the furnace (Fig. 5(b)). The above reasons weaken the effect of $T_{\text{sec air}}$ on $T_{\text{fefg}}$, resulting in no obvious effect of $T_{\text{sec air}}$ on the superheater. Therefore, the above two limitations cannot form real constraints about elevating $T_{\text{sec air}}$. Then, in this paper, the $T_{\text{sec air}}$ will be elevated to explore the performance of the S-$CO_2$ coal-fired power system.

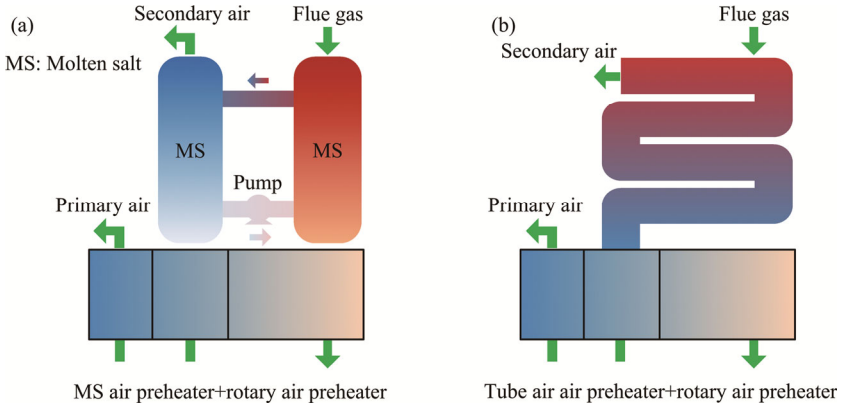


**Fig. 4** Two types of high-temperature air preheater

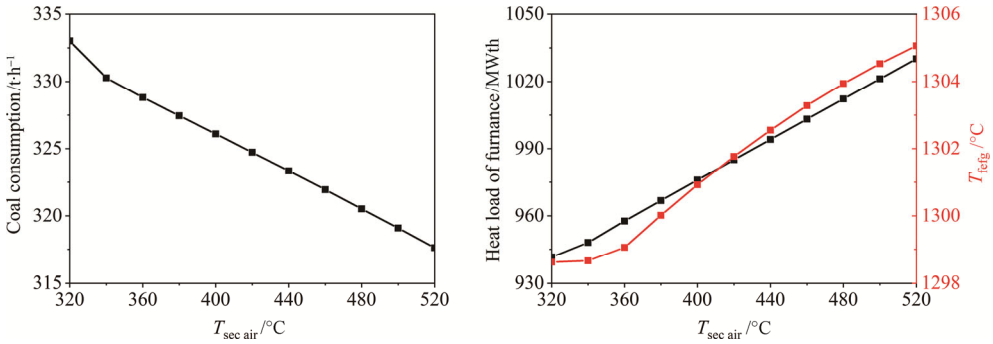


**Fig. 5** The influence of $T_{\text{sec air}}$ on coal consumption, heat load of furnace, and $T_{\text{fefg}}$

## 4. The Main Vapor Pressure Adjustment Method

The parameters adjustment method adjusts the main vapor pressure $P_5$ of the S-$CO_2$ cycle and the secondary air temperature $T_{\text{sec air}}$. A criterion is needed to have zero residual flue gas heat, $Q_{\text{re}}$=0. Combining Eqs. (12), (17) and (18) yields the following criterion.

$$T_4 = T_{\text{sec air}} + \Delta T_{\text{p,air}} - \Delta T_{\text{p,4}} \tag{21}$$

Eq. (21) shows constant difference between $T_4$ and $T_{\text{sec air}}$ (see Fig. 6(a)). The core concept of the main vapor pressure adjustment method is to vary $P_5$ to achieve suitable $T_4$ to satisfy the criterion given in Eq. (21). Because the main vapor temperature $T_5$ is important to influence the system performance, Fig. 6(b) plots $T_4$ versus $T_5$ at $T_{\text{sec air}}$ =400°C, 450°C and 500°C, respectively. The selection of the three secondary air temperatures satisfies $T_{\text{sec air}}$<531.9°C shown in Section 3. Fig. 6(b) shows that $T_{\text{sec air}}$ and $P_5$ obviously influence the range of $T_5$. In Fig. 6(b) $T_4$ is kept unchanged by adjusting $P_5$. The corresponding $P_5$ is shown in Fig. 7(a). To ensure the complete absorption of the flue gas heat, when the main vapor pressure is given, a lower secondary air temperature requires to decrease both the $CO_2$ temperatures entering and leaving the boiler ($T_4$ and $T_5$). Inversely, a higher secondary air temperature elevates both $T_4$ and $T_5$. On the other hand, when the secondary air temperature is fixed, $P_5$ influences the $T_5$ range, due to the constraint of $P_5$ in the range of 20-50 MPa (see Tab. 1). For example, the $CO_2$ temperature entering the boiler is $T_4$=399°C at $T_{\text{sec air}}$=400°C (see

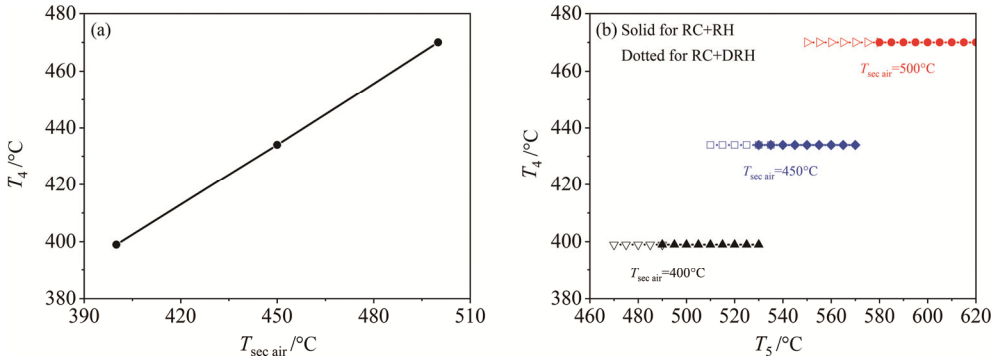


**Fig. 6** The relationship between $T_4$ and $T_{sec\ air}$ (a) and the effect of reheating/double-reheating and main vapor temperatures on such relationship (b)

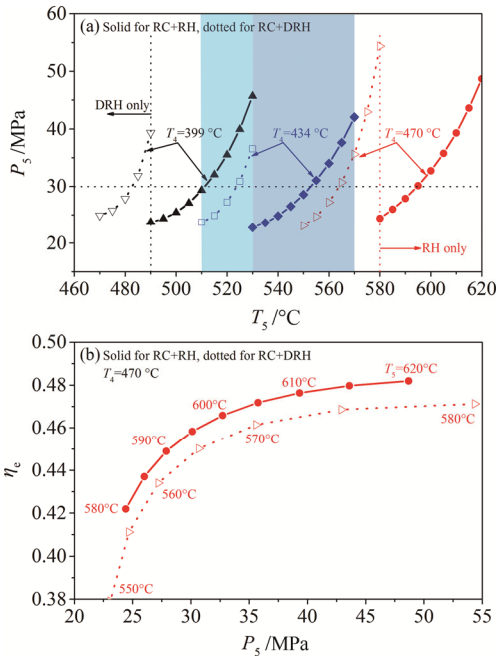


**Fig. 7** The relationship between $P_5$ and $T_5$ to satisfy $Q_{re}$=0 (a) and power generation efficiencies versus $P_5$ and $T_5$ (b)

Fig. 6(a)). To keep $T_4$=399°C, the $P_5$ range of 24.92-39.36 MPa shall correspond to the $T_5$ range of 470-490°C for RC+DRH cycle to ensure $Q_{re}$=0.

To ensure $Q_{re}$=0, the main vapor pressure $P_5$ should be adjusted to a specific value to adapt a given main vapor temperature $T_5$, so that the relationship between $T_4$ and $T_{sec\ air}$ given in Eq. (21) can be satisfied. Thus, there exists a relationship between main vapor pressure $P_5$ and main vapor temperature $T_5$, which is presented at different $T_4$ (or $T_{sec\ air}$) for single-reheating and double-reheating (see Fig. 7(a)). Single-reheating (RH) is only available for higher main vapor temperatures in the range of 580–620°C, due to restriction on $P_5$. On the other hand, for lower $T_5$ in the range of 470–490°C, double-reheating (DRH) is preferable. In this $T_5$ range, using of single-reheating results in low main vapor pressure to obviously deteriorate power generation efficiency. At moderate $T_4$ (or $T_{sec\ air}$), single-reheating yields higher main vapor temperatures (see blue region in Fig. 7(a)), and double-reheating corresponds to lower main vapor temperatures (see light-blue region in Fig. 7(a)). Fig. 7(b) plots power generation efficiencies $\eta_e$ versus main vapor pressures $P_5$ for RC+RH and RC+DRH. It is observed that single-reheating behaves obviously higher efficiency than double-reheating. At $P_5$=48.68 MPa, $\eta_e$ are 48.20% and 47.05% for single-reheating and double-reheating, respectively.

In summary, at given main vapor temperature and secondary air temperature, a main vapor pressure can be searched to ensure no residual flue gas heat. Thus, this strategy is called the main vapor pressure adjustment method. Single-reheating is suitable for higher main vapor temperatures, and behaves better thermal performance than double-reheating.

## 5. The FGC method

The core concept of the FGC method is to arrange an additional heat exchanger in tail flue to absorb the flue gas heat in middle temperature range. Fig. 8(a-b) shows the RC+RH+FGC and RC+DRH+FGC configurations. For both single-reheating and double-reheating, a small $CO_2$ flow rate is extracted from the compressor C1 outlet, which is heated by flue gas and finally returns to the cycle at the HTR inlet. Correspondingly, the *T–s* diagrams are shown in Fig. 8(c) for single-reheating and Fig. 8(d) for double-reheating.

It is recognized that for supercritical water-steam Rankine cycle power plant, double-reheating improves cycle efficiency. This conclusion should be revisited for S-$CO_2$ cycle. Surprisingly, it is found that both single-reheating and double-reheating result in identical power generation efficiency (see Fig. 9(a)). The difference between single-reheating (RH) and double-reheating (DRH) is that DRH creates larger residual flue gas heat ($Q_{re}$) than RH (see Fig. 9(b)). The secondary air

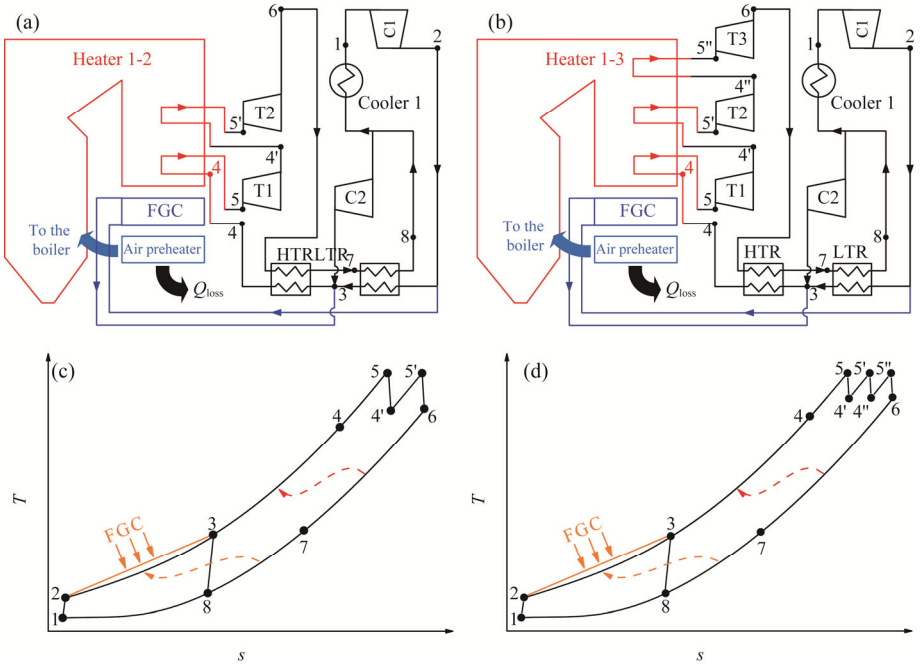


**Fig. 8** S-$CO_2$ cycle with FGC (a and c for single-reheating, b and d for double-reheating)

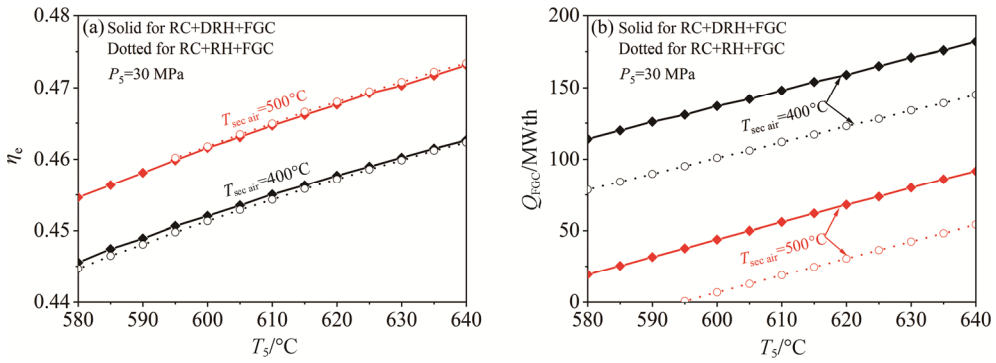


**Fig. 9** Effect of single and double reheating on $\eta_e$ and $Q_{FGC}$ versus $T_5$

temperatures also influence residual flue gas heat. The lower the secondary air temperature, the larger residual flue gas heat appears. Smaller heat is received by air preheater at lower secondary air temperature to leave more residual flue gas heat. In order to explain the similar power generation efficiency for RH and DRH when FGC is used, the thermal efficiency is written as

$$\eta_{th} = \frac{\sum W_t - \sum W_c}{Q_{h,cycle} + Q_{FGC}} \tag{22}$$

Because residual flue gas heat is larger for DRH than RH, the using of double-reheating turns to deteriorate system thermal efficiency, accounting for similar power generation efficiency for both RH and DRH. Because single-reheating not only has simpler cycle configuration, but also creates smaller residual flue gas heat, it is better than double-reheating when the FGC method is used.

We conclude that single-reheating is better than double-reheating. The comparison between the main vapor pressure adjustment method and the FGC method focusses on single-reheating (see Fig. 10). The power

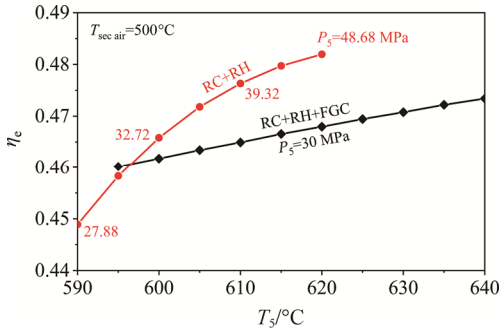


**Fig. 10** The comparison of main vapor pressure adjustment method and FGC method on the power generation efficiencies

generation efficiency curves are crossing between the two methods. The crossing point occurs at $T_5$=596.5°C and $\eta_e$=46.04%. Because the main vapor temperature is relatively low at the crossing point, the operation at the crossing point is not practical for modern power plant. Beyond the crossing point, the main vapor pressure adjustment method holds larger power generation efficiency than the FGC method, and the efficiency difference becomes larger when the main vapor temperatures are increased. For the main vapor pressure adjustment method, the power generation efficiency is $\eta_e$=48.2% at $T_5$=620°C and $P_5$=48.68 MPa. For the FGC method, $\eta_e$ equals to 46.8% at $T_5$=620°C and $P_5$=30 MPa.

It is known that the system performance can be improved by raising main vapor temperatures, which is especially true for supercritical water-steam Rankine cycle system. For Rankine cycle, the ultra-high pressure may cause wet-steam expansion in turbine to yield serious water erosion on turbine blades. Thus, the main vapor pressure adjustment method is not suitable for Rankine cycle. However, wet-steam expansion cannot occur in a S-$CO_2$ cycle system because the turbine operates in supercritical pressure region. The main vapor pressure adjustment method for S-$CO_2$ coal fired power plant has following benefits: (1) obviously higher power generation efficiency; (2) dry-expansion in turbine; (3) simple system design without FGC and double-reheating. One shall note that higher pressure will influence the structure load, material creep and component lifetime, which should be further investigated. From the operation and economic consideration, the main vapor pressure adjustment method is a promising strategy for S-$CO_2$ coal fired power plant, if the system pressure can be higher than conventional.

## 6. Conclusions

The following conclusions can be drawn:

A comprehensively theoretical model was developed in this paper, including thermodynamics, boiler pressure drops and energy distribution in various components in the system.

Because the secondary air temperature ($T_{sec\ air}$) determines residual flue gas heat, the maximum secondary air temperature is theoretically determined based on energy conservation between flue gas and air, which is 531.9°C for the coal used in this paper. The secondary air temperature weakly influences the flue gas temperature at furnace exit for higher $T_{sec\ air}$, which can be further increased with the new modification of air preheater.

The main vapor pressure adjustment method searches a suitable main vapor pressure adapting to a specific main vapor temperature, so that the residual flue gas heat becomes zero at given secondary air temperature. Single-reheating is suitable for higher main vapor temperature and behaves apparently higher efficiency than double-reheating.

If residual flue gas heat does exist, the residual flue gas heat is recovered by FGC. Single-reheating and double-reheating share identical power generation efficiency, but single-reheating creates smaller residual flue gas heat.

It is concluded that single-reheating is better than double-reheating for both the main vapor pressure adjustment method and the FGC method. The main vapor pressure adjustment method is promising for S-$CO_2$ coal fired power plant.

## Acknowledgements

This paper is supported by the National Key R&D Program of China (2017YFB0601801), the Science Fund for Creative Research Groups of the National Natural Science Foundation of China (51821004), the Fundamental Research Funds for the Central Universities (2018ZD02 and 2018QN042).

## References

[1] Moisseytsev A., Sienicki J.J., Investigation of alternative layouts for the supercritical carbon dioxide Brayton cycle for a sodium-cooled fast reactor. Nuclear Engineering and Design, 2009, 239(7): 1362–1371.

[2] Ahn Y., Lee J.I., Study of various Brayton cycle designs for small modular sodium-cooled fast reactor. Nuclear Engineering and Design, 2014, 276: 128–141.

[3] Jeong W.S., Lee J.I., Jeong Y.H., Potential improvements of supercritical recompression $CO_2$ Brayton cycle by mixing other gases for power conversion system of a SFR. Nuclear Engineering and Design, 2011, 241(6): 2128–2137.

[4] Li M., Zhu H., Guo J., Wang K., Tao W., The development technology and applications of supercritical $CO_2$ power cycle in nuclear energy, solar energy and other energy industries. Applied Thermal Engineering, 2017, 126: 255–275.

[5] Wang K., He Y., Thermodynamic analysis and optimization of a molten salt solar power tower integrated with a recompression supercritical $CO_2$ Brayton cycle based on integrated modeling. Energy Conversion and Management, 2017, 135: 336–350.

[6] Wang X., Liu Q., Lei J., Han W., Jin H., Investigation of thermodynamic performances for two-stage recompression supercritical $CO_2$ Brayton cycle with high temperature thermal energy storage system. Energy Conversion and Management, 2018, 165: 477–487.

[7] Kim M.S., Ahn Y., Kim B., Lee J.I., Study on the supercritical $CO_2$ power cycles for landfill gas firing gas turbine bottoming cycle. Energy, 2016, 111: 893–909.

[8] Kim Y.M., Sohn J.L., Yoon E.S., Supercritical $CO_2$ Rankine cycles for waste heat recovery from gas turbine. Energy, 2017, 118: 893–905.

[9] Hou S., Wu Y., Zhou Y., Yu L., Performance analysis of the combined supercritical $CO_2$ recompression and regenerative cycle used in waste heat recovery of marine gas turbine. Energy Conversion and Management, 2017, 151: 73–85.

[10] Angelino G., Carbon dioxide condensation cycles for power production. Journal of Engineering for Power, 1968, 90(3): 287–295.

[11] Dostal V., A supercritical carbon dioxide cycle for next generation nuclear reactors. Nuclear Engineering, Massachusetts Institute of Technology, Cambridge, USA, 2004.

[12] Holcomb G.R., Carney C., Doğan Ö.N., Oxidation of alloys for energy applications in supercritical $CO_2$ and $H_2O$. Corrosion Science, 2016, 109: 22–35.

[13] Zhong D.W., Meng J.A., Qin P., et al., Effect of cooling water flow path on the flow and heat transfer in a 660 MW power plant condenser. Journal of Thermal Science, 2019, 28(2): 262-270.

[14] International Energy Agency (IEA). Key world energy statistics 2017, 2017.

[15] BP statistical review of world energy June 2017. https://www.bp.com/en/global/corporate/energy-economics/statistical-review-of-world-energy.html, 2017.

[16] Gonzalez-Salazar M.A., Kirsten T., Prchlik L., Review of the operational flexibility and emissions of gas- and coal-fired power plants in a future with growing renewables. Renewable and Sustainable Energy Reviews, 2018, 82: 1497–1513.

[17] Xu J., Sun E., Li M., Liu H., Zhu B., Key issues and solution strategies for supercritical carbon dioxide coal fired power plant. Energy, 2018, 157: 227–246.

[18] Sun E., Xu J., Li M., Liu G., Zhu B., Connected-top-bottom-cycle to cascade utilize flue gas heat for supercritical carbon dioxide coal fired power plant. Energy Conversion and Management, 2018, 172: 138–154.

[19] Hanak D.P., Manovic V., Calcium looping with supercritical $CO_2$ cycle for decarbonisation of coal-fired power plant. Energy, 2016, 102: 343–353.

[20] Zhou J., Zhang C., Su S., Wang Y., Hu S., Liu L., et al., Exergy analysis of a 1000 MW single reheat supercritical $CO_2$ Brayton cycle coal-fired power plant. Energy Conversion and Management, 2018, 173: 348–358.

[21] Chen S., Soomro A., Yu R., Hu J., Sun Z., Xiang W., Integration of chemical looping combustion and supercritical $CO_2$ cycle for combined heat and power generation with $CO_2$ capture. Energy Conversion and Management, 2018, 167: 113–124.

[22] Le Moullec Y., Conceptual study of a high efficiency coal-fired power plant with $CO_2$ capture using a supercritical $CO_2$ Brayton cycle. Energy, 2013, 49: 32–46.

[23] Mecheri M., Le Moullec Y., Supercritical $CO_2$ Brayton cycles for coal-fired power plants. Energy, 2016, 103: 758–771.

[24] Park S., Kim J., Yoon M., Rhim D., Yeom C., Thermodynamic and economic investigation of coal-fired power plant combined with various supercritical $CO_2$ Brayton power cycle. Applied Thermal Engineering, 2018, 130: 611–623.

[25] Lemmon E.W., Huber M.L., Mc Linden M.O., NIST standard reference database 23: reference fluid thermodynamic and transport properties-REFPROP, version 9.1. Tech. rep., National Institute of Standards and Technology, Standard Reference Data Program, Gaithersburg, 2013.

[26] Liu Z., He Y., Yang Y., Fei J., Experimental study on heat transfer and pressure drop of supercritical $CO_2$ cooled in a large tube. Applied Thermal Engineering, 2014, 70(1): 307–315.

[27] Basu P., Kefa C., Jestin L., Boilers and burners: design and theory. Springer Science & Business Media, New York, 2012.

[28] Chen H., Pan P., Shao H., Wang Y., Zhao Q., Corrosion and viscous ash deposition of a rotary air preheater in a coal-fired power plant. Applied Thermal Engineering, 2017, 113: 373–385.

[29] Wang L., Deng L., Tang C., et al., Thermal deformation prediction based on the temperature distribution of the rotor in rotary air-preheater. Applied Thermal Engineering, 2015, 90: 478–488.

[30] Zhao L., Zhou Q., Boiler course design. China Electric Power Press, Beijing, 2013 (in Chinese).